Available online at www.sciencedirect.com
SCIENCE DIRECT®
Journal of Sound and Vibration 268 (2003) 993–1012
JOURNAL OF SOUND AND VIBRATION
www.elsevier.com/locate/jsvi

# Finite element model updating of a small scale bridge

J.L. Zapico[a,*], M.P. González[a], M.I. Friswell[b], C.A. Taylor[c], A.J. Crewe[c]

[a] *Department of Construction and Manufacturing Engineering, University of Oviedo, Campus de Viesques 7.1.16, 33203 Gijón, Spain*

[b] *Department of Aerospace Engineering, University of Bristol, Queen's Building, University Walk, Bristol BS8 1TR, UK*

[c] *Department of Civil Engineering, University of Bristol, Queen's Building, University Walk, Bristol BS8 1TR, UK*

Received 9 April 2002; accepted 28 November 2002

**Abstract**

Although considerable experience has been gained in model updating, the critical issues that remain are the choice of parameters and how to deal with ill-conditioning. Although a number of theoretical tools exist to help with both of these tasks, the techniques are advancing by gaining experience with a diverse range of structures. This paper adds to this debate by updating an experimental bridge model with a geometric scale of 1:50 that represents a typical multi-span continuous-deck motorway bridge. The bridge has four identical straight spans and an irregular distribution of piers, and the central pier is shorter than the others. Four configurations corresponding to different pier stiffnesses and the inclusion of an isolation–dissipation device were considered. An initial test without the piers present was also performed. The measurement of data in these different configurations allows the model updating to be performed sequentially, where parameters identified in earlier configurations maintain their estimated values in subsequent configurations. This approach means that each configuration has a small number of uncertain parameters to be identified, leading to a set of well-conditioned estimation problems based on predicting four natural frequencies of the structure. The procedure was successful, and all of the measured natural frequencies were estimated accurately with a maximum error of under 2.5%.


## 1. Introduction

This paper is concerned with modelling the response of bridges under transverse seismic loading. The approach taken is to estimate uncertain parameters of the model by testing the structure in a variety of different configurations in order to overcome the ill-conditioning often

*Corresponding author. Tel.: +34-985-181-928; fax: +34-985-182-055.

*E-mail addresses:* jzapico@correo.uniovi.es (J.L. Zapico), placeres@correo.uniovi.es (M.P. González), m.i.friswell@bristol.ac.uk (M.I. Friswell), colin.taylor@bristol.ac.uk (C.A. Taylor), a.j.crewe@bristol.ac.uk (A.J. Crewe).

0022-460X/03/$ - see front matter 
doi:10.1016/S0022-460X(03)00409-7

inherent in updating complex structures. The approach is demonstrated on a small-scale irregular bridge model that was intended to approximately reproduce both the linear response of the bridge under minor earthquakes and the non-linear response due to severe earthquakes. In this paper only the linear response is considered. The tests were performed within the European Consortium of Earthquake Shaking Tables (ECOEST), which was financed by Human Capital and Mobility Program of the European Commission, and helped to update Eurocode 8, which aims to combine theory and experiment [1]. Modal and seismic tests on the experimental structure were performed at the Earthquake Engineering Research Center within the University of Bristol [1]. The PREC8 project also included shaking table tests performed in Lisbon (LNEC) and Bergamo (ISMES) and pseudo-dynamic tests performed in Ispra (JRC-ELSA) with large-scale models. The prototype used in these tests was also used in this work in order to allow the results to be compared. The aim of the prototype design was to be representative of typical multi-span continuous-deck motorway bridges [1–3].

The deck of the bridge had the form of a hollow-core post-tensioned concrete girder, with a full scale width of 14 m. The deck was designed to end at the abutments with shear keys so as to allow the extremities to rotate. The bridge had four identical straight spans of 50 m each. The deck was connected to the piers by bearings in both the vertical and transverse directions. The bridge was intentionally highly irregular, and the first mode of the structure is very different to that of the deflected shape of the deck alone. The three piers were respectively 14, 7 and 21 m high (see Fig. 1), and had rectangular hollow-core reinforced concrete sections. Concrete C25 and steel A500 were used in the design of the bridge. Four different configurations labeled as A, B, C and D were adopted. Bridge A was designed according to the current version of Eurocode 8, Part 2. Bridge B was similar to A but with increased reinforcement in the short pier which aims to decrease its ductility demand. Bridge C was also similar to A but with increased reinforcement in the higher piers. Finally, bridge D was similar to A but with isolation–dissipation devices over the short pier where the demands are concentrated for the conventionally designed structure. The prototype isolation–dissipation device was essentially composed of vertical ductile steel spindles with non-uniform cross-section, which act as cantilever vertical beams [3].

Theoretical studies on simplified models were also carried out, which tried to match the linear seismic response to the experimental ones. The comparison of the modal properties of these theoretical models to the corresponding experimental ones revealed large differences. A first attempt at improving the model by trial and error was attempted, however, significant differences remained that meant the models were unable to accurately reproduce the response of the bridge. The objective of this work was to develop a systematic procedure to update the linear elastic finite

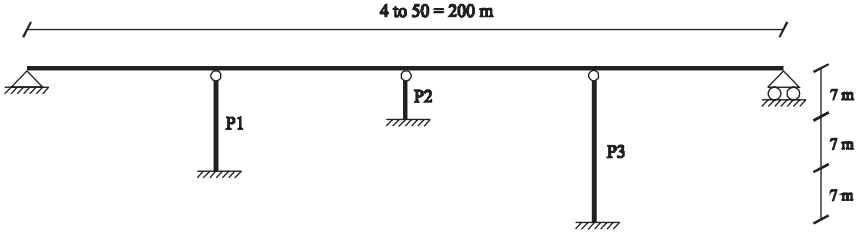


Fig. 1. General scheme of the bridge.

element model, so that the updated physical properties could be used to predict the linear response.

## 2. Experimental model

The model scaling was mainly conditioned by the characteristics of the earthquake simulator. A geometric scale factor of 50 has been adopted, so as not to exceed the maximum available length of the shaking table, which is 5 m. A so-called weight distorted or artificial mass simulation model was chosen, with the acceleration scale factor set equal to one [4]. Table 1 summarizes the other scale factors used in the modelling. The adopted geometric scale meant that the materials used for the model had to be different from those of the prototype. Structural steel BS 4368 grade 43c was chosen instead of post-tensioned concrete for the model deck, and aluminum alloy grade 6082 T6 which was annealed after machining was chosen instead of reinforced concrete for the model piers.

### 2.1. Supports

The main support of the bridge was designed with a $200 \times 200$ mm, 8 mm thick, square hollow section, which is appropriate to resist the torsional and bending moments that occur during the test. The support was intended to replicate the shape of the valley spanned by the bridge. Three intermediate vertical supports were also added, and these supports had very stiff universal columns that were bolted to the main support. Underneath the main support, directly under the vertical supports, welded plates were used to clamp the support to the shaking table (Figs. 2 and 3). In order to increase the transverse stiffness, the ends of the main support and the top of the vertical support corresponding to the short pier were braced to the table by means of channel sections.

### 2.2. Deck

The model deck was designed with a continuous square hollow section. A $60 \times 60$ mm, 3.2 mm thick section was used, that had a similar second moment of area to that required for similarity

Table 1
Scaling factors for the model similarity

| Scaling factors | |
|---|---|
| Length ($N_h$) | 50 |
| Acceleration ($N_{\ddot{y}}$) | 1 |
| Time ($N_t$) | $(N_h/N_{\ddot{y}})^{1/2} = 7.07$ |
| Curvature ($N_c$) | $1/N_h = 0.02$ |
| Angular force ($N_{AF}$) | $5.21 \times 10^5$ |
| Linear force ($N_{LF}$) | $N_{AF}/N_h = 10\,432$ |
| Mass ($N_M$) | $N_{LF}/N_{\ddot{y}} = 10\,432$ |

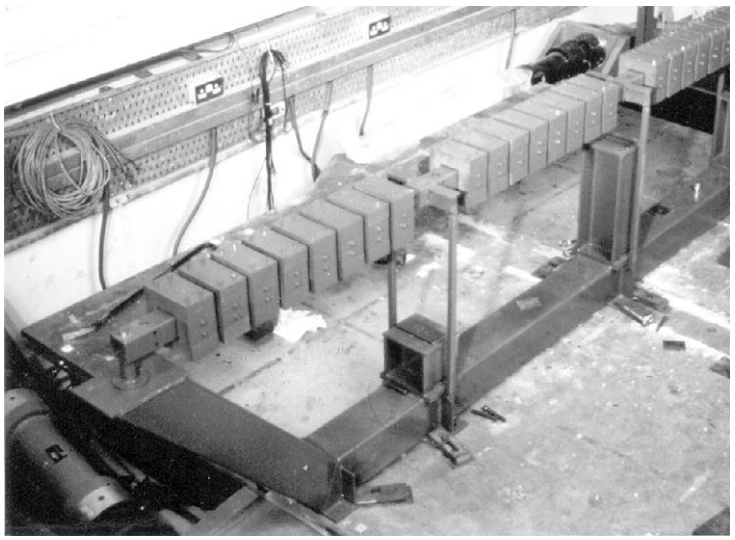

Fig. 2. Photograph of the model set-up.

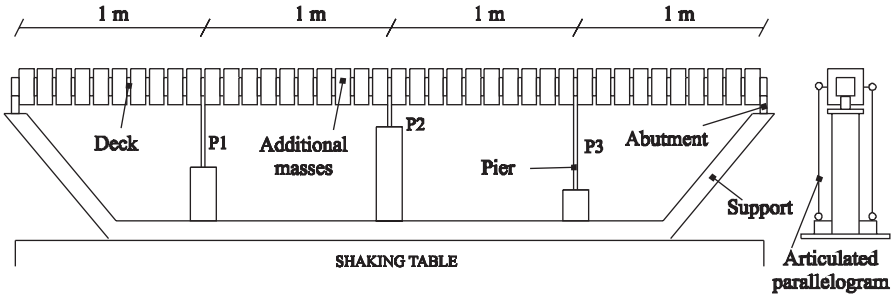


Fig. 3. Elevation of the experimental model.

between the prototype and model (Figs. 2 and 4). In order to attain mass similarity, additional masses were added to the model. These additional masses were distributed along the deck (Fig. 3). Each additional mass was formed with four steel blocks that were bolted to each other and positioned around the deck so that the center of gravity of the deck was not changed. Each additional mass was attached to the deck by two bolts, and both bolts were set in the same transverse section so as not to distort the bending stiffness of the deck (Fig. 4). The additional mass required is relatively large and this extra weight would cause a significant static vertical deflection. Articulated parallelograms are attached to the deck at the pier locations (Figs. 2 and 3) that constrain the deck to translate only in the horizontal direction. These parallelograms are stiff vertically to support the weight of the deck but provide little stiffness in the transverse direction, which is of interest in the experiment. Supporting the deck only at the pier locations provided sufficient vertical stiffness and the parallelograms were used in all configurations. Furthermore, the parallelograms prevent torsional vibrations of the deck due to the eccentricity of the connections to the piers.

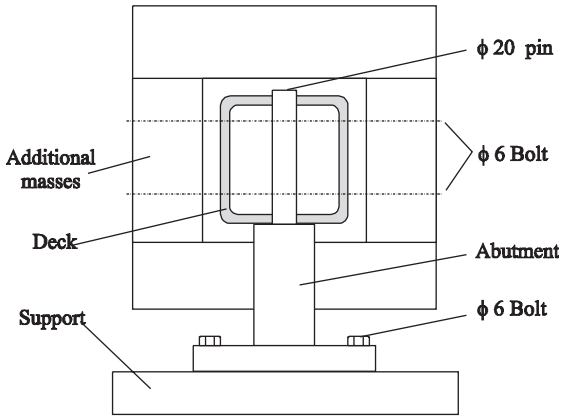


Fig. 4. Additional masses and connection of the abutments to the deck and the support.

Table 2
Distribution and dimensions of the model piers (mm)

| Configuration | Pier | *h* | *b* | *t* |
|---|---|---|---|---|
| A,D | P1 | 34.0 | 20.1 | 1.8 |
| | P2 | 33.2 | 23.4 | 2.2 |
| | P3 | 33.6 | 20.8 | 1.8 |
| B | P1 | 34.0 | 20.1 | 1.8 |
| | P2 | 31.7 | 31.8 | 2.9 |
| | P3 | 33.6 | 20.8 | 1.8 |
| C | P1 | 32.5 | 26.6 | 2.5 |
| | P2 | 34.4 | 19.4 | 1.7 |
| | P3 | 32.1 | 27.6 | 2.5 |

### 2.3. Piers

The piers were designed with an I-beam section at the bottom, and a rectangular section for the remainder. Both sections had the same depth and width for each pier (Fig. 4). This design was intended to approximately reproduce the response of the prototype piers under vertical and transverse loads, acting simultaneously. Table 2 shows the dimensions of the different piers computed by the similarity laws.

### 2.4. Connections and the dissipation device

The deck ends hinged on the abutments through two vertical pins 20 mm in diameter. The abutments were bolted to the main support by four bolts 6 mm in diameter (Figs. 2 and 4). All of the piers had the same type of connection to the support including four 6 mm diameter bolts (Fig. 5). The connections to the deck were also the same for all piers and consisted of square keys

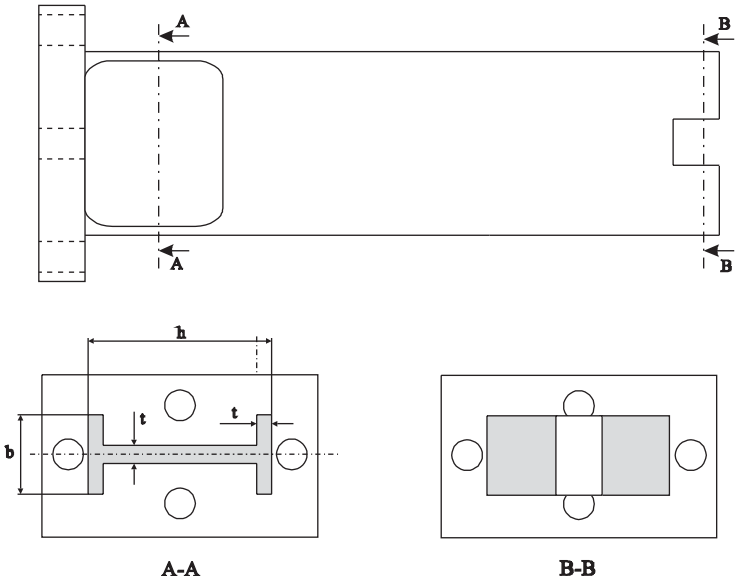


Fig. 5. Details of the piers.

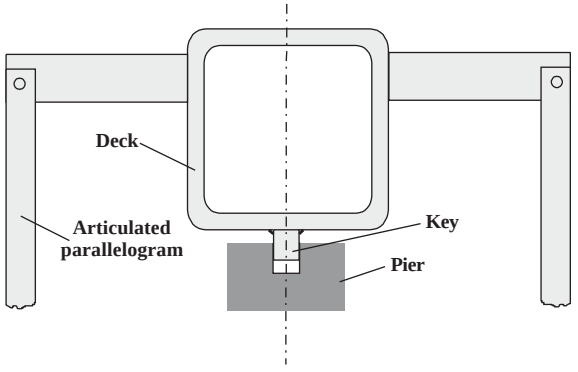


Fig. 6. Connection of the piers to the deck.

welded to the deck that fitted into slots in the piers (Fig. 6). This ensured that the weight of the deck was taken by the main support rather than the piers. The isolation–dissipation device was designed as a single spindle of structural steel and was welded to the deck and pinned to the top of the shorter pier (Fig. 7). The device is flexible and elastic for small displacements and acts as a cantilever beam fixed to the deck. For large displacements (not considered here) the device yields and thus dissipates energy.

## 3. Testing

The model was set up on the shaking table and experimental modal testing was initially performed on the deck alone without piers. This additional configuration was labeled as T, and it

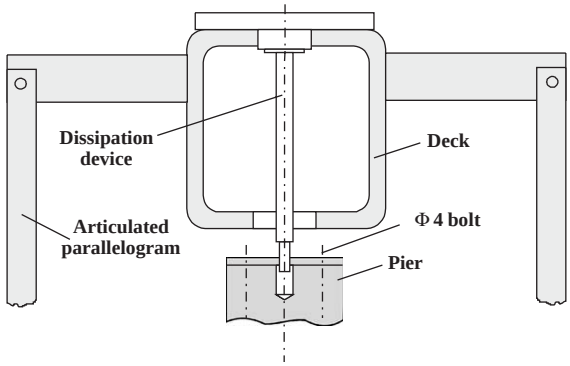


Fig. 7. Details of the isolation–dissipation device.

was only used for updating purposes. Afterwards, configurations A, B, C and D were tested in turn. In each configuration, an initial modal test followed by several seismic tests was carried out.

In the modal tests, the model was directly excited in the transverse direction by the shaking table with a low intensity random vibration. The response of the model was measured by an accelerometer that was placed at different positions on the deck and support using a magnetic base. At each position, the frequency response functions (FRFs) over the range 0–50 Hz were obtained by averaging ten measurements, and the modal model extracted. Table 3 shows the first four measured natural frequencies for the different configurations. The second mode was poorly identified in configuration T due to the proximity of some accelerometer placements to nodal points and the frequency interval used in the FRFs. Consequently, the second mode of configuration T was rejected in the following analysis and the fifth mode was used instead.

The model was also shaken in the transverse direction in the seismic tests. The experiments excited the bridge with a series of earthquakes with the same shape but increasing intensity, namely: 0.3, 0.5, 0.8, 1.0, 1.2 and 2.0 times the design intensity. The reference earthquake was an artificial one fitting the Eurocode 8 elastic response spectrum for medium soil conditions [5], had a maximum acceleration of 0.35 g and a duration of 13 s at full scale. During these tests the displacement of the deck at the connection to the piers relative to the table was measured by means of linear variable differential transformers. Additionally, the absolute acceleration at the same points was measured using accelerometers.

## 4. Finite element models

Several spatial finite element models composed of beams were developed to simulate the transverse dynamic behavior of the bridge, for configurations A, B, C and D. Another configuration, T, that represents the bridge deck alone without piers was also modelled.

In these models, the deck of the bridge was modelled by 44 Timoshenko beam elements with identical mechanical properties and connected in series. Nodes were placed at the abutments, the pier locations and the points of attachment of the additional masses. Two additional elements were attached at the ends of the deck to represent the elastic behavior of the abutments. These elements consisted of small length (0.01 m) beams perpendicular to the deck. The connection of

Table 3
Natural frequencies (Hz) of the 1:50 scale bridge

| Configuration | Mode | Finite element model | | | | Experimental model | Error % | |
|---|---|---|---|---|---|---|---|---|
| | | Initial | Updated T | Updated ABC | Updated D | | Initial | Final |
| T | 1 | 2.5679 | 2.8978 | | | 2.89 | −11.15 | 0.27 |
| | 3 | 22.8523 | 21.3026 | | | 21.16 | 8.00 | 0.67 |
| | 4 | 39.8616 | 34.6849 | | | 35.12 | 13.50 | −1.24 |
| | 5 | 62.1422 | 49.8493 | | | 49.39 | 25.82 | 0.93 |
| A | 1 | 12.1816 | 12.1604 | 11.6554 | | 11.60 | 5.01 | 0.48 |
| | 2 | 14.9646 | 14.8733 | 13.3637 | | 13.60 | 10.03 | −1.74 |
| | 3 | 30.0128 | 28.0831 | 25.8306 | | 25.75 | 16.55 | 0.31 |
| | 4 | 39.5075 | 34.7048 | 34.7003 | | 35.00 | 12.88 | −0.86 |
| B | 1 | 12.2665 | 12.2402 | 11.7591 | | 11.85 | 3.51 | −0.77 |
| | 2 | 15.6035 | 15.4453 | 13.7890 | | 13.85 | 12.66 | −0.44 |
| | 3 | 32.2059 | 30.0429 | 26.6944 | | 26.10 | 23.39 | 2.28 |
| | 4 | 39.5075 | 34.7045 | 34.7003 | | 35.00 | 12.88 | −0.86 |
| C | 1 | 12.4451 | 12.4222 | 11.7188 | | 11.65 | 6.82 | 0.59 |
| | 2 | 15.1855 | 15.1148 | 13.4900 | | 13.65 | 11.25 | −1.17 |
| | 3 | 28.6850 | 26.8408 | 25.2395 | | 25.15 | 14.06 | 0.36 |
| | 4 | 39.5109 | 34.7147 | 34.7041 | | 35.00 | 12.89 | −0.85 |
| D | 1 | 8.0457 | 8.1647 | 7.7455 | 8.0003 | 8.00 | 0.57 | 0.00 |
| | 2 | 12.7668 | 12.7360 | 12.1865 | 12.1943 | 12.50 | 2.13 | −2.45 |
| | 3 | 23.9608 | 22.4606 | 22.3117 | 22.3960 | 22.40 | 6.97 | −0.02 |
| | 4 | 39.5102 | 34.7043 | 34.7003 | 34.7003 | 35.00 | 12.89 | −0.86 |

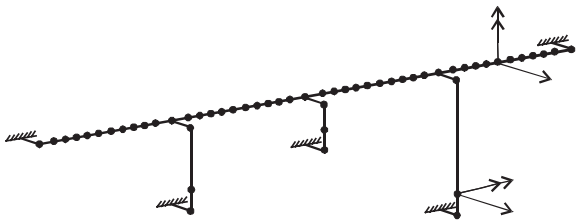

Fig. 8. Finite element model.

the deck to the piers and the isolation–dissipation device were also modelled with additional elements similar to those of the abutments. The degrees of freedom (DOFs) considered in the deck were the horizontal transversal translation and the rotation around a vertical axis. A consistent uniformly distributed mass was assumed for the deck, while the additional masses were lumped at the corresponding nodes and accounted for both the mass and moment of inertia.

The piers were modelled by two Timoshenko beam elements corresponding each to the rectangular top section and the I-shaped bottom one. Only the degrees of freedom corresponding to the horizontal transversal translation and the rotation around the horizontal axis were

retained. The connection of the piers to the ground was also simulated with small length elements perpendicular to the piers. A consistent, uniformly distributed mass was used.

The models were coded in MATLAB using the *Structural Dynamics Toolbox* [6,7], and are illustrated in Fig. 8.

## 5. Comparison of numerical and experimental modal results

As a first approximation, the connections of the deck to the abutments and the piers were modelled as perfect hinges. This was simulated in the numerical model by choosing a cross-section with high area and a low second moment of area for the additional elements. The area of the additional element simulating the isolation–dissipation devices was selected so that its flexibility was equal to that of the design device. The connections of the piers to the ground were modelled as completely rigid, and were simulated in the numerical model by choosing high area and second moment of area for the corresponding additional elements.

The computed natural frequencies based on these initial finite element models are shown in Table 3 along with those obtained experimentally. The natural frequencies from the model were always higher than those obtained by experiment, with up to 25.82% error, except for the first mode of configuration T which was 11.15% lower. All of the configurations show the same trend: the higher the natural frequency, the higher the error.

## 6. Model updating

Model updating is now quite a mature technology [8–10]. The techniques have moved away from direct approaches that reproduce the measured modal data, to methods based on optimization that allow a range of measurements and physical parameters to be used. Thus much of the emphasis in model updating is concerned with the choice of parameters, and methods to reduce the ill-conditioning in the resulting equations [11]. The procedure of updating adopted will now be described, and consists of three successive steps outlined in the following sections.

### 6.1. Choice of updating parameters

The choice of the updating parameters is critical to improve the modelling of the bridge. Physical properties of the elements such as Young's modulus and mass density, or geometric properties such as area and second moment of area of the cross-section, nodal positions, or the stiffness of the connections, could be chosen as updating parameters. In practice, however, the discrepancies between the experimental and analytical models are mainly due to a few parameters. On the other hand, the available modal data used to update the model is incomplete, only the lower modes can be identified and they contain uncertainties due to measurement and identification errors. Under these conditions, the selection of suitable parameters for each case is a difficult task that cannot be automated and requires considerable engineering insight and intuition [8].

As a general rule, only parameters that the response is sensitive to should be selected, otherwise the updating process will be ill-conditioned since insufficient information is available to estimate the parameters accurately. Among these parameters, only those having physical meaning should be updated, otherwise the updated model may reproduce the data used for updating but might not accurately predict the response of the bridge under different conditions. Furthermore, there should be some expectation that the parameters chosen are likely to be in error. Sometimes the parameters corresponding to several elements are expected to have similar values. In these cases one super-element parameter should be selected rather than individual element parameters.

In this work, only a few updating parameters were selected on the basis of the prior knowledge about the dynamic behavior of the bridge and the analysis of the discrepancies between the experimental and analytical models. They were tried in turn until a reasonable convergence to the experimental data was reached in each configuration.

### 6.2. Initial parameter values

Initial values of the parameters are required for the finite element model. They should be selected to be as close as possible to the actual values so that the subsequent optimization process will find the solution quickly, and the chances of finding a local minimum are reduced. The nominal values of some physical properties of the model, such as mass density, Young's modulus, dimensions of cross-sections, etc., are approximately known a priori, and the experimental deviations from these are relatively small.

However, there is a little information about the values of the actual rotational stiffness of the connections used in the models. The stiffness is between $\infty$, corresponding to a completely rigid connection, and 0, corresponding to a perfectly hinged connection. Furthermore, there is usually only a small range of stiffness where the response of the structure changes from that predicted by these extreme stiffnesses. To overcome this problem and to achieve an appropriate initial value, the following procedure based on modal sensitivity is proposed. An error function $\varepsilon$ is defined as the distance of the vector containing the experimental natural frequencies, $f^{\mathrm{e}}$, from the vector containing the corresponding analytical frequencies, $f^{\mathrm{a}}$, as

$$\varepsilon = \sum_{i=1}^{4} \left( \frac{f_i^{\mathrm{a}} - f_i^{\mathrm{e}}}{f_i^{\mathrm{e}}} \right)^2. \tag{1}$$

This function is weighted by the inverse of the experimental natural frequencies so as to normalize the contribution of each mode to the total error. The variation of this error as a function of each connection stiffness is then obtained numerically for an interval that includes the expected actual stiffness. The linear stiffness is expected to be in the range $10^{-2}$–$10^{15}$ N/m, where the lower limit corresponds to a very flexible connection, while the upper limit corresponds to a stiff connection. The range for angular stiffness is assumed to be 1–$10^{10}$ Nm.

Fig. 9 shows the error surface corresponding to configuration T as a function of the linear and angular stiffness of the abutments. There is a flat zone for high values of the linear stiffness and low values of the angular stiffness, and beyond this plateau there is a valley where the error diminishes. Along this valley, the error function is almost constant for low values of the angular stiffness. As the angular stiffness is increased the error function reaches a minimum, then increases

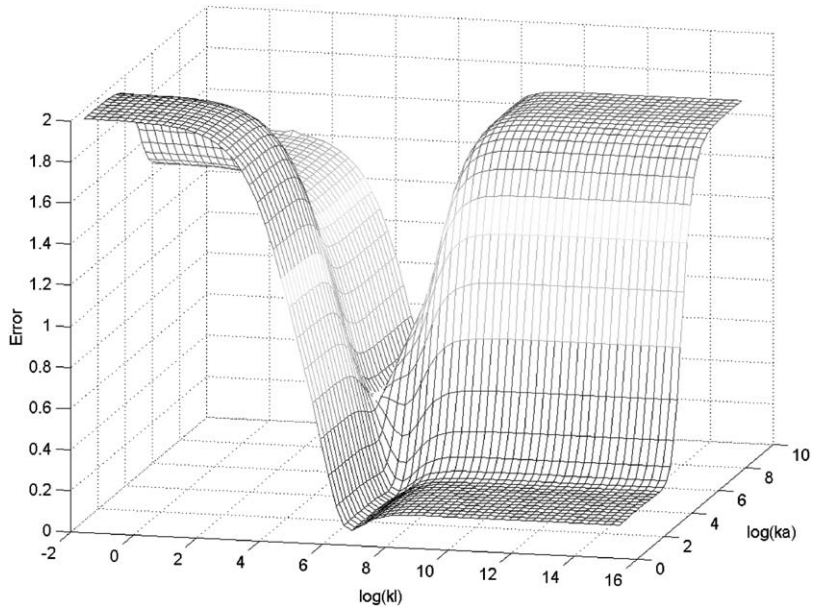


Fig. 9. Weighted error as a function of the linear and angular stiffness ($K_l$ and $K_a$) of the abutments (Configuration T).

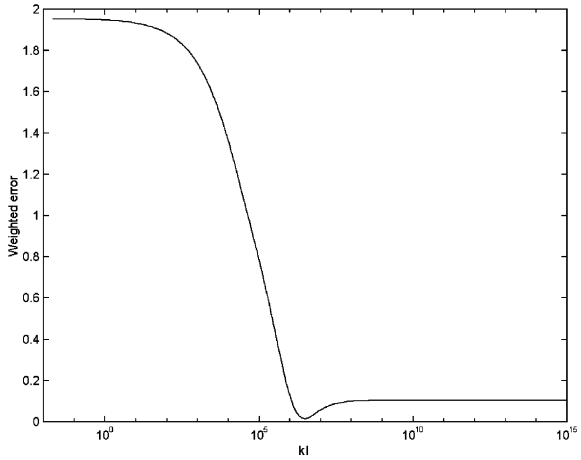


Fig. 10. Variation of the weighted squared error as function of the linear stiffness of the abutments (Configuration T).

steeply and finally becomes flat. The values of the parameters corresponding to the minimum error are selected as initial parameters. The cross-sections of the error surface at the minimum are shown in Figs. 10 and 11, and the flat zones and minimum error are clearly evident in these plots. Similar shapes of the error function results were found for the other configurations considered in this paper.

If the value of the parameters were selected in the flat zones, the subsequent process of optimization would be slowed down considerably or might lead to an incorrect solution. This selection of initial parameters is essentially a model updating exercise performed on a limited set of the uncertain parameters.

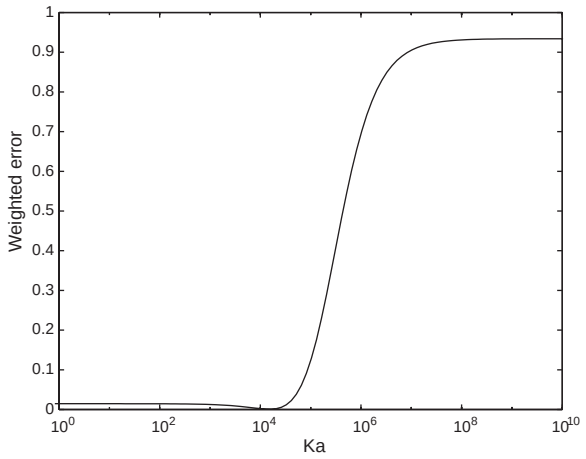


Fig. 11. Variation of the weighted squared error as function of the angular stiffness of the abutments (Configuration T).

### 6.3. Model updating procedure

Once the significant parameters and their starting values have been selected, they are simultaneously optimized by minimizing the error function defined by Eq. (1). For this purpose, the multivariate function *fminsearch* within the *Optimization Toolbox* of MATLAB [7] was used. This function uses the Nelder–Mead simplex algorithm [12], which is one of the most widely used methods for non-linear unconstrained optimization. This method attempts to minimize a scalar-valued non-linear function of $n$ real variables using only function values, without any explicit or implicit derivative information. Thus, the Nelder–Mead method falls into the general class of direct search methods.

At each step the method maintains a non-degenerate simplex, that is a geometric figure in $n$ dimensions of non-zero volume that is the convex hull of $n+1$ vertices. Each iteration begins with the simplex from the previous iteration, which is specified by its $n+1$ vertices and the associated function values. The worst and best vertices are defined as those having the highest and lowest value of the scalar function. The simplex is optimized through a reflection, expansion and contraction of the worst vertex of the simplex or by shrinking the previous simplex around the best vertex. The process ends when the difference between successive values of the scalar function is lower than a given threshold, $10^{-4}$ in this case. The method is very robust and does not depend on calculating derivatives or the continuity of the function. However, the method does need more iterations to converge than other methods.

### 6.4. Updating results

The application of the updating procedure to the different configurations of the model is detailed in the following subsections. The updating is performed sequentially, so that, for example, the parameters estimated in configuration T are fixed when the other configurations are modelled.

*6.4.1. Configuration T*

Model updating starts with this configuration because it allows the deck model to be improved without the uncertainties arising from the pier modelling. The first physical property selected for updating was the bending stiffness of the deck, $EI_s$. The uncertainty in this bending stiffness was due to geometric imperfections of the sections, the reductions due to the holes and variations in the mechanical properties of the material. Nevertheless, no significant relative variations of the bending stiffness were expected between the elements of the deck because it was manufactured from a continuous bar. Thus all of the elements in the deck were assumed to have the same stiffness and hence a single super-element parameter was selected. A starting value of $EI_s = 79\,722\,\mathrm{Nm}^2$ was adopted, which corresponds to the nominal value of Young's modulus of the structural steel, $E = 2.06 \times 10^5\,\mathrm{MPa}$, and the nominal second moment of area of the cross-section, $I = 3.87 \times 10^{-7}\,\mathrm{m}^4$.

However, the updating results were poor when only the bending stiffness was updated. This is because a variation of the bending stiffness leads to the same relative variation in all of the natural frequencies, while the relative differences between the initial FE model and the experimental results increase with frequency, as has been pointed out in Section 5. Therefore, the updating should be refined by including another physical parameter of the bridge. One possibility is to include the transverse stiffness of the abutments, which include the stiffness of the abutments themselves and their connection to the support. This connection was assumed to be rigid in the initial FE model, but it is well known that there is always some degree of flexibility in practice. However, better results are obtained by including the stiffness of the elements corresponding to the abutments, since the higher the natural frequency the higher the displacement of the abutments (see Fig. 12), and hence the larger the influence of the abutment stiffness.

Even after including this second parameter, some significant error still remains in the lower modes. One source of this error may be the boundaries conditions. Indeed, the connections of the deck to the abutments were modelled as perfect hinges in the initial FE model, but they may have some angular stiffness due to friction. The natural frequency predictions were improved by including this angular stiffness in the model.

The linear and angular stiffnesses of the abutments were modified by varying the area and second moment of area of the corresponding additional elements. It was assumed that both abutments have the same linear and angular stiffnesses $K_l$ and $K_a$, which constitute the parameters to be updated. As there is no previous estimate of this stiffness, the error in the response of the model given by Eq. (1), was computed as a function of $K_l$ and $K_a$, at the initial flexural stiffness of the deck, $EI_s$. Figs. 9–11 show the results. The calculated values corresponding to the minimum error are $K_l = 3.27 \times 10^6\,\mathrm{N/m}$ and $K_a = 1.64 \times 10^4\,\mathrm{Nm}$, which were selected as the initial parameter values.

The updated parameters were then obtained by minimizing the error function, using the Simplex method mentioned earlier. Table 4 shows the updated parameters, along with the corresponding residual squared error. The highest change from the initial FE model corresponds to the linear and angular stiffnesses of the abutments, from infinite to $3.11 \times 10^6\,\mathrm{N/m}$ and from zero to $1.69 \times 10^4\,\mathrm{Nm}$. The bending stiffness of the deck only reduces by about 1.8%. Table 3 shows the natural frequencies computed using the updated parameters together with the corresponding measured frequencies for comparison. The four natural frequencies are all correct to within an error of 1.24%.

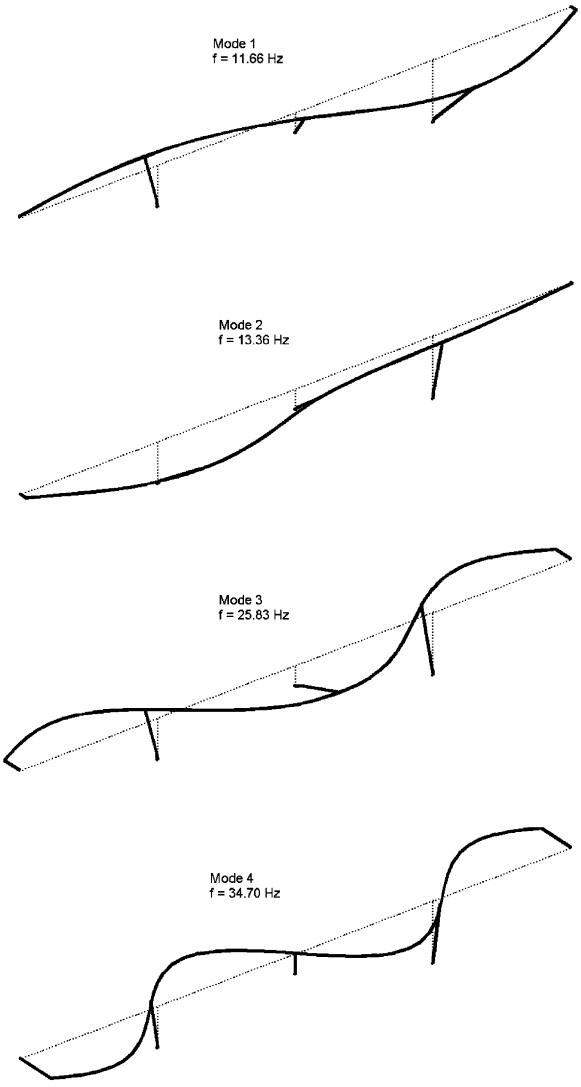


Fig. 12. Normal mode shapes for the updated configuration A.

Table 4
Updating parameters (Configuration T)

| Parameter | $EI_s$ (Nm$^2$) | $K_l$ (N/m) | $K_a$ (Nm) | Error ($\varepsilon$) |
|---|---|---|---|---|
| Starting | $7.97 \times 10^4$ | $3.27 \times 10^6$ | $1.64 \times 10^4$ | — |
| Updated | $7.83 \times 10^4$ | $3.11 \times 10^6$ | $1.69 \times 10^4$ | $3.20 \times 10^{-4}$ |

The natural frequencies for configurations A, B, C and D were also computed using the updated parameters obtained above, and are given in Table 3, labeled as 'Updated T'. Significant improvement was obtained in the natural frequency estimates for these configurations, just by

updating the deck and abutment stiffnesses. The fourth simulated natural frequency is very close to the corresponding experimental frequencies in all of the configurations. This is because the pier has little influence on this mode shape (see Fig. 12).

*6.4.2. Configurations A, B, C*

The parameters updated using the T configuration were maintained at the values estimated in Section 6.4.1. Even after updating using the T configuration, significant errors remain for modes 1, 2 and 3 (see Table 3) and the frequencies predicted by the model are higher than those obtained experimentally. These errors might be due to boundary conditions and consequently the flexural stiffness of the connections between the piers and the supports were selected for updating. Although the piers have different cross-sections, all of them have the same connection to the support and hence the flexural stiffness of the connections is assumed to be equal for all of the piers and all of the configurations. The connection stiffness was changed in the FE model by modifying the second moment of area of the corresponding additional elements.

Young's modulus of the piers, $E_a$, was the second physical property selected for updating in configurations A, B and C. In this case, Young's modulus is an equivalent parameter that affects the total stiffness of the piers. The second moment of area of the piers was rejected as a parameter because the piers were accurately manufactured and so the cross-sectional properties are unlikely to be in error. Moreover, changes in the actual second moment of area from the design values are expected to be random and their updated values would be affected by the experimental modal data errors, which are also random.

In this case, the error function was extended to include the three configurations and the first four modes simultaneously. Thus,

$$\varepsilon = \sum_{j=A,B,C} \sum_{i=1}^{4} \left( \frac{f_{i,j}^{a} - f_{i,j}^{e}}{f_{i,j}^{e}} \right)^2 . \tag{2}$$

Since Young's modulus of the piers and the stiffness of the connections are assumed to be the same for configurations A, B and C, there are two unknown parameters to estimate from the 12 measured natural frequencies. The initial value for $E_a$ was $7 \times 10^4$ MPa, which is the nominal value for the aluminum used. The initial value for the stiffness of the connections was $K_p = 1.04 \times 10^5$ Nm, which was obtained by the procedure explained in Section 6.2. The analysis of the error function reveals that in a large interval around its minimum value the response of the model is quite insensitive to Young's modulus of the piers. Consequently, this parameter was rejected in the updating process and the nominal value adopted for the remainder of the analysis.

The minimization of the error function yielded the updating parameter given in Table 5. The stiffness of the connections changed only slightly, showing that the initial value was a good

Table 5
Updating parameters (Configuration ABC)

| Parameter | $K_p$ (Nm) | Error ($\varepsilon$) |
|---|---|---|
| Starting | $1.04 \times 10^5$ | — |
| Updated | $1.04 \times 10^5$ | $1.40 \times 10^{-3}$ |

Table 6
Updating parameters (Configuration D)

| Parameter | $K_d$ (N/m) | Error ($\varepsilon$) |
|---|---|---|
| Initial | $3.53 \times 10^5$ | — |
| Updated | $4.13 \times 10^5$ | $6.71 \times 10^{-4}$ |

estimate. The natural frequencies predicted by the finite element model with the updated parameters are shown in Table 3, labeled as 'Updated ABC', and compared to the corresponding experimental frequencies. Most of the frequencies have absolute differences below 1% and the maximum difference is 2.28%.

### 6.4.3. *Configuration D*

The isolation–dissipation device included in this configuration has been modelled through the additional element connecting the deck to the central pier, and its stiffness is changed by varying the area of the additional element. The selected updating parameter was the stiffness of this isolation–dissipation device, $K_d$, with the initial value being taken as the design value. The error function included the first four natural frequencies. The updated parameter and predicted natural frequencies were obtained using an approach similar to the previous configurations. The initial and updated parameters are shown in Table 6, and the predicted and measured natural frequencies are compared in Table 3. The discrepancies in natural frequencies for this configuration are all below 2.45%, with three below 0.9%.

## 7. Validation

The strategy adopted in this work was to select as few as possible updating parameters in each configuration, and once estimated they are fixed for the following configurations. This gives confidence that the obtained solution has physical meaning. If many parameters are selected, there are several combinations of the their values that lead to local minima of the error function, i.e., the solution is not unique and has no physical meaning. By updating the models sequentially only one minimum of the error surface exists for all the configurations studied, and this gives some confidence that the number of selected parameters is appropriate.

On the other hand, each configuration of the bridge constitutes an extension of the previous ones. For example, configuration D can be obtained from the configuration A by introducing a flexible connection between the deck and the short pier. Similarly, configuration A can be formed from the configuration T by adding the piers. Thus, if a combination of parameters fits the experimental data well but it has no physical meaning, it would be unable to reproduce the response of the bridge under different conditions. It was found that the parameters updated in each configuration improved the response of the model in the subsequent configurations, and no further modification to the parameter was needed. Configurations A, B and C were simultaneously updated using a single parameter, namely the stiffness of the connections of the

piers. This suggests that the corrected parameters should give good predictions under other untested conditions.

Nevertheless, an independent demonstration of the validity of the updated model was performed by taking advantage of the available data measured during the seismic tests. For this purpose, the low intensity tests were used, where a linear response was expected. The time history of the measured displacements of the deck at the connection to the piers was compared with those predicted by the models. Neglecting the dissipative forces the response of the bridge to the seismic loading can be modelled in the time domain by the following linear elastic, time invariant spatial model

$$[\mathbf{M}]\{\mathbf{a}(t)\} + [\mathbf{K}]\{\mathbf{x}(t)\} = \{0\}, \tag{3}$$

where $[\mathbf{M}]$ is the mass matrix, $[\mathbf{K}]$ is the stiffness matrix, $\{\mathbf{a}\}$ is the absolute acceleration vector and $\{\mathbf{x}\}$ is the displacement relative to the table. Thus, the displacements predicted by the model $\{\hat{\mathbf{x}}\}$ on the basis of the measured absolute accelerations $\{a_m\}$ are

$$\{\hat{\mathbf{x}}(t)\} = -[\mathbf{K}]^{-1}[\mathbf{M}]\{a_m(t)\}. \tag{4}$$

The mass and stiffness matrices were obtained from those of the FE model using the system equivalent reduction expansion process (SEREP) [8], and the reduced model reproduces exactly the three lower frequencies of the full model. This process was applied to both the initial and the updated models in all the configurations and the displacements predicted by Eq. (4) were compared with those measured in the tests. Fig. 13 shows the early part of a typical measured displacement together with the predictions of both the initial and updated models. The predictions of the updated model are much closer to the measurements than the predictions of the initial model.

In order to obtain an overall comparison of the measured and predicted response of the bridge, two different indices were defined and calculated. The first index is the proportional regression coefficient (PRC), which was obtained by applying proportional regression using least squares to the time histories of the measured and the predicted displacements. This index represents the

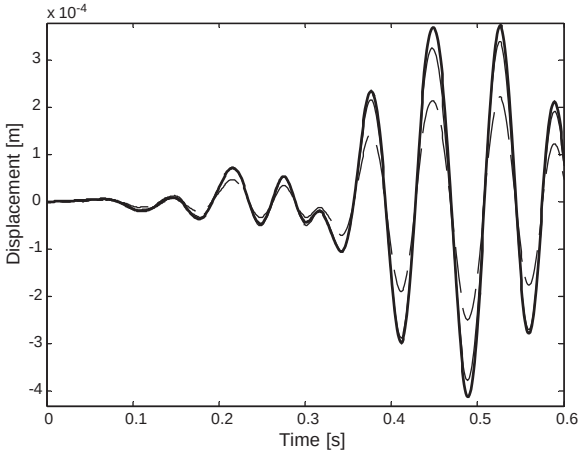


Fig. 13. Time history of the displacements of the pier P2 (Configuration A). —— Measured. – – – Initial model. - - - Updated model.

accuracy of the numerical model to reproduce the physical response, and characterizes the systematic errors in the numerical model. The closer the PRC is to one, the higher the accuracy of the numerical model, i.e. the lower the systematic errors. The second index is the residual to signal ratio (RSR), which is the quotient of the standard deviation of the residuals to that of the measured signal. In this case the residuals are defined as the difference between the predictions and measurements. The RSR is a measure of the precision of both the measurements and the predictions of the model.

The above indices were computed using both the initial and the updated models for configurations A, B, C and D at the measured degrees of freedom, and Tables 7–10 show the results. The values of the PRC for the initial model (Table 7) are relatively low, especially for configurations A, B and C, which means that the initial models have low accuracy. However, the PRCs for the updated models (Table 8) are close to one and show that the updated models are much more accurate. The RSR for the updated models is also an improvement over the initial models in all configurations and measured degrees of freedom. The values corresponding to the updated model are between 5% and 15%. These results demonstrate the capacity of the updated model to reproduce the dynamic response of the bridge under conditions different to those used for the updating.

Table 7
Proportional regression coefficient. Initial models

| | A | B | C | D |
|---|---|---|---|---|
| P1 | 0.87 | 0.82 | 0.82 | 0.91 |
| P2 | 0.61 | 0.51 | 0.62 | 0.86 |
| P3 | 0.89 | 0.83 | 0.86 | 0.90 |

Table 8
Proportional regression coefficient. Updated models

| | A | B | C | D |
|---|---|---|---|---|
| P1 | 1.02 | 0.98 | 0.99 | 1.01 |
| P2 | 0.92 | 0.87 | 0.88 | 0.87 |
| P3 | 0.99 | 0.94 | 0.96 | 0.91 |

Table 9
Residual to signal ratio. Initial models

| | A | B | C | D |
|---|---|---|---|---|
| P1 | 0.15 | 0.21 | 0.19 | 0.12 |
| P2 | 0.39 | 0.49 | 0.38 | 0.15 |
| P3 | 0.17 | 0.22 | 0.17 | 0.14 |

Table 10
Residual to signal ratio. Updated models

| | A | B | C | D |
|---|---|---|---|---|
| P1 | 0.05 | 0.10 | 0.05 | 0.11 |
| P2 | 0.09 | 0.15 | 0.13 | 0.15 |
| P3 | 0.09 | 0.14 | 0.09 | 0.14 |

The values of the final PRCs are slightly lower than one, especially for the central pier, P2. This means that the predicted displacements are lower than the measured ones, and Eq. (4) shows that the updated stiffness is too high. This could be due to some local plastic behavior at the bottom and connection of the piers, especially in the short pier, during the seismic tests, since the displacements are larger than in the modal tests.

The values of the PRCs for the initial configuration D are higher than the other configurations and close to the corresponding updated configuration. A possible explanation is that the earthquake excites mainly the first mode in this configuration due to the presence of the isolation–dissipation device, and there is a small difference between the first mode of the initial and updated models (see Table 3). In the configurations A, B, and C, however, this is not the case, leading to lower values of PRCs in configurations A, B and C.

## 8. Conclusions

The study of the small-scale bridge model has shown that the stiffness of the connections has a high influence on its modal properties. It has been demonstrated that both the selection of updating parameters and also the setting of initial parameter values is crucial to the success of an iterative model updating scheme. A procedure based on modal sensitivity is proposed to find the appropriate initial values of the unknown parameters. The updated models were able to accurately predict the measured natural frequencies of the bridge and also its response under low intensity seismic tests, which allowed the validation of the updated model.

More generally, this paper has demonstrated the advantage of estimating parameters using different configurations. Configuration T consisted of the deck alone, and allowed parameters relating to the deck to be updated without errors introduced by the pier modelling. Configurations A, B and C allowed the pier model to be improved, using the deck parameters identified from the measurements of configuration T. Configuration D allowed the model of the isolation–dissipation device to be improved using the previously identified deck and pier models. The approach may be used more generally for a wide range of structures that are built up from components, and this paper has demonstrated its effectiveness in estimating accurate models of complete structures. The experience could be applied to full scale bridges, allowing the stiffness of the connections and the foundations, which are generally either unknown or difficult to model, to be estimated using the lower natural frequencies. For a real bridge, clearly it would be impossible to perform all of the tests outlined in this paper, however valuable modelling information may be gained from tests during construction.

## Acknowledgements

This work has been developed under the ECOEST2 network project under the Human Capital and Mobility Program of the European Commission. The experimental part was performed at the Earthquake Engineering Research Center (EERC) of the University of Bristol. The collaboration of the EERC staff, particularly Professor Severn, is greatly acknowledged.

## References

[1] R.T. Severn, European experimental research in earthquake engineering for Eurocode 8, Proceedings of the Institution of Civil Engineers Structures & Bridges 134 (1999) 205–217.
[2] V.A. Pinto, Pseudo-dynamic and shaking table tests on RC bridges, Report No. 5, ECOEST & PREC8, 1996.
[3] V.A. Pinto, G. Verzeletti, P. Pegon, G. Magonette, P. Negro, J. Guedes, Pseudo-dynamic testing of large-scale R/C bridges, Report EUR 16378 EN, ELSA, Ispra, Italy, 1996.
[4] W.E. Baker, P.S. Westine, F.T. Dodge, Similarity Methods in Engineering Dynamics, Elsevier Science Publisher B.V., The Netherlands, 1991.
[5] Eurocode 8, Design of structures for earthquake resistance, Part1: general rules, seismic actions and rules for building. Doc CEN/TC250/SC8/N269, Draft No. 1, 2000.
[6] E. Balmès, Structural Dynamics Toolbox, Scientific Software Group, 1997.
[7] Matlab, Users Manual Version 5.2, The Math Works, Inc., 1998.
[8] M.I. Friswell, J.E. Mottershead, Finite Element Model Updating in Structural Dynamics, Kluwer Academic Publishers, Dordrecht, 1995.
[9] J.E. Mottershead, M.I. Friswell, Model updating in structural dynamics: a survey, Journal of Sound and Vibration 167 (2) (1993) 347–375.
[10] J.E. Mottershead, M.I. Friswell (Guest Eds.), Inverse methods in structural dynamics, Special Issue of Mechanical Systems and Signal Processing 15(1) (2001).
[11] M.I. Friswell, J.E. Mottershead, H. Ahmadian, Finite element model updating using experimental test data: parameterisation and regularisation, Proceedings of the Royal Society of London, Series A: Mathematical, Physical and Engineering Sciences 359 (2001) 169–186.
[12] J.A. Nelder, R. Mead, A simplex method for function minimisation, Computer Journal 7 (1965) 308–313.